Available online at www.sciencedirect.com

ScienceDirect

Procedia CIRP 135 (2025) 456–461

www.elsevier.com/locate/procedia

32nd CIRP Conference on Life Cycle Engineering (LCE 2025)

Comparative Environmental Impact Analysis of Friction-based Additive Manufacturing Techniques

Simone Amantia[a], Kirill Kalashnikov[a], Giuseppe Ingarao[a, *], Rosa Di Lorenzo[a], Gianluca Buffa[a], Livan Fratini[a]

[a]*Department of Engineering, University of Palermo, Viale delle Scienze, Palermo, 90128, Italy*

* Corresponding author. Giuseppe Ingarao *E-mail address:* giuseppe.ingarao@unipa.it

Abstract

In this work, two variants of solid-state friction-based additive processes, Friction Surfacing Deposition and Friction Stir Additive Manufacturing, were compared in terms of their environmental impact. A comparative Life Cycle Assessment analysis was performed, alongside experimental quantification and analysis of energy and resource flows for each process. The energy analysis revealed that the friction stir additive manufacturing is a more energy-consuming technology than surfacing process due to the significantly lower tool feed rate required to produce sound welds. It was determined that the most significant contributor to the environmental impact of both methods is the process scrap. Strategies to reduce material waste were proposed for each technology, tailored to the specific characteristics of their implementation. Furthermore, an additional LCA model was developed to evaluate strategies for minimizing FSAM process scrap.

Keywords: FSD; FSAM; AM; LCA; Aluminum;

1. Introduction

The metal 3D printing in manufacturing processes has been widely used for several years. Thanks to the high flexibility of 3D printing approaches, there have been numerous and rapid developments. Currently, Additive Manufacturing (AM) techniques are widely used in various sectors such as aerospace, biomedical, automotive, and energy [1]. The most widespread techniques for metals are Laser Beam Melting (LBM), Electron Beam Melting (EBM), and Laser Metal Deposition (LMD). Although these techniques have been under the research spotlight over the last few years, they still have some issues, as they are based on fusion welding techniques [2].

The use of these processes with light alloys, such as titanium, aluminum, and magnesium, results in the formation of metallurgical defects. These defects include an elevated susceptibility to cracking and the development of porosity, which are unavoidable consequences of the melting and solidification processes involved. To overcome these issues, some studies have been turned to AM techniques based on solid-state joining [3]

In this regard, two categories of processes are mainly investigated by researchers: Friction Stir Additive Manufacturing (FSAM) and Friction Stir Deposition (FSD) [4][5]. These methods can provide improved structure and mechanical properties compared to fusion-based Metal Additive Manufacturing (MAM) techniques. Both technologies

10.1016/j.procir.2024.12.043

can use the same equipment, from the modified milling machines to the specially designed Friction Stir Welding (FSW) ones, and the FSAM process requires tools as those utilized in standard FSW [6]. More than that, the process parameters selection and assessment of feasibility for both processes have already been performed [7] [8].

The analysis of literature shows that the FSD technology can operate with a wide range of metallic materials, such as high-strength martensitic steels, heat-treatable and non-heat-treatable aluminum alloys, as well as titanium and other alloys, which makes it promising for various industrial applications [9]. This is possible since the tool is consumable, so the process depends only on the physical-mechanical properties of the raw material. At the same time, the FSAM process depends on the configuration of the welding system, especially on the FSW-tool material and geometry, and the thickness of workpieces [10]. Despite that, it is shown that using the proper design of experiments, including the tool configuration, it is possible to produce additive components from different non-ferrous alloys with high operational performance [11]. However, while both methods can effectively fabricate metallic components, it's crucial to also consider other aspects of technologies, such as lead time, energy costs, and material waste, to fully comprehend the efficiency of a process.

In recent years, several works have been carried out about the analysis of the environmental impact of AM processes, such as WAAM techniques [12][13], thanks to which it has been possible to formalize a robust methodology for the environmental impact analysis of these technologies [14].

Although solid-state-based Additive manufacturing could provide a solution for specific applications, these processes are characterized by a large amount of process scrap and, above all, their environmental impact has not been analyzed yet.

The present paper aims to start covering this research gap and presents a LCA comparative analysis of FSD and FSAM processes to uncover the strengths and weaknesses of such processes in terms of their environmental impact.

Nomenclature

AM	Additive Manufacturing
SLM	Selective Laser Melting
EBM	Electron Beam Melting
FSAM	Friction Stir Additive Manufacturing
FSD	Friction Surfacing Deposition
FSW	Friction Stir Welding
LMD	Laser Metal Deposition
LCA	Life Cycle Assessment
MAM	Metal Additive Manufacturing
UFG	Ultrafine-grained
WAAM	Wire Arc Additive Manufacturing
HAZ	Heat Affected Zone
CED	Cumulative Energy Demand

2. Methods and Materials

A dedicated Friction Stir Welding machine, ESAB Legio, was used to carry out the processes with different setups for the two methods. For the manufacturing phases, the electrical energy absorbed by the ESAB was recorded using Chauvin Arnoux C.A. 8331, connected to the input of the machine.

A backing plate with 6 mm thickness made of AA5083-H111 with 175 mm x 75 mm dimensions was used for both analyzed processes.

FSD process was carried out as follows: AA2011-T3 consumable tool with 25 mm of diameter and 67 mm of height was fixed in the welding head of the machine. Then, it was pressed onto a substrate with a loading force of 9 kN under a rotation rate of 840 rpm and moved along the welding line with a speed of 370 mm/min to create a material layer by the principles of direct metal transfer.

Figure 1 shows a schematic representation of the process. The green arrows indicate vertical load, while the orange line represents the feeding direction.

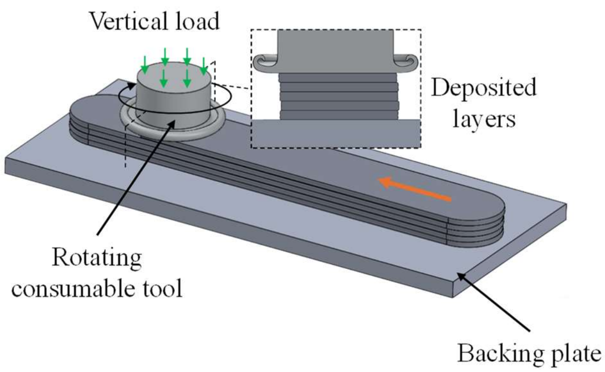

Fig. 1. FSD process.

The wall manufacturing consists of several deposition steps (one consumable tool is used for each step), followed by machining operations to remove the allowance.

As far as the FSAM technique is regarded, the pinless approach is analysed as it appears to be the most environmentally friendly solution of this process category (see Figure 2).

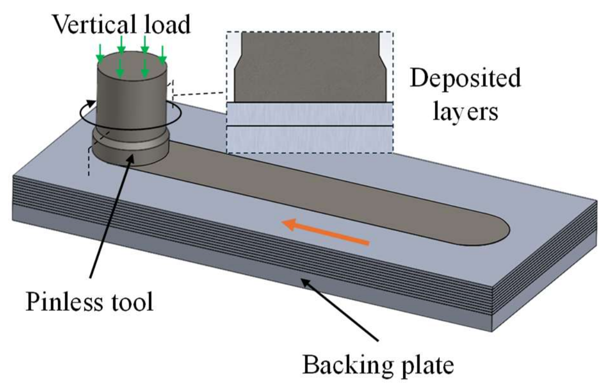

Fig. 2. FSAM process.

FSAM process was carried out by layer-by-layer welding of thin metal sheets. In contrast to FSD method, this technology utilizes a welding tool and the principles of solid bonding. To perform the process, two sheets were fixed on the working table and then welded with a specific loading force, feed rate, and rotation speed. In the current work, a set of 1 mm thick sheets was used to allow a pinless approach. The high-performance steel pinless tool with a diameter of 25.0 mm was used for the processing under conditions of 6 kN of loading force, 80 mm/min of feed rate, and 1100 rpm of tool rotation rate.

After the welding of each layer, a milling operation is carried out, in the same machine and without unclamping the build, to eliminate the small flash at the sides of the weld seam and guarantee good contact conditions for the next layer.

After piling the required number of metal sheets up, final machining operations are needed to cut off the parts of the sheet used for clamping (see Figure 3b).

It is worth noting that, after the processing phase of FSAM, only 14 mm width of the welded layer will be considered for the comparative analysis. The dimensions of the starting metal sheets were 175 mm x 75 mm x 1 mm (L x W x H).

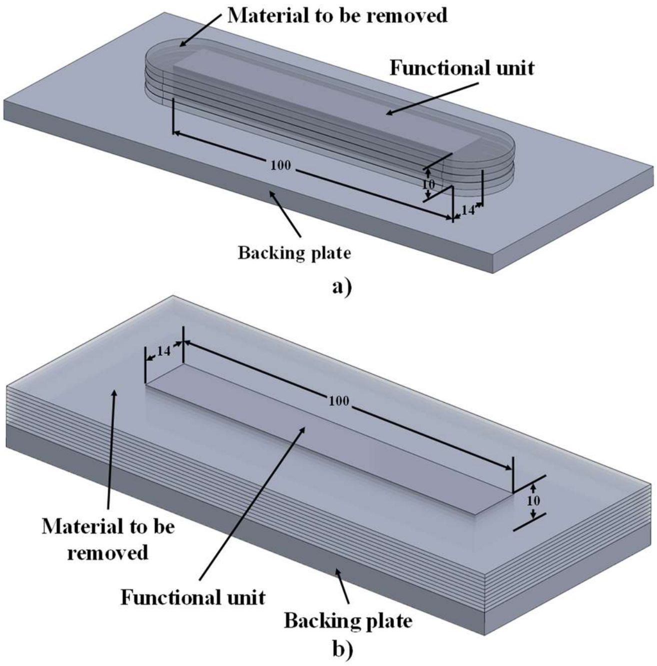

Fig. 3. Functional unit in FSD specimen.

3. Comparative LCA analysis

Following the ISO 14040/44, a specific Life Cycle Assessment (LCA) analysis and a comparative LCA analysis were modeled. ILCD guidelines [15] were taken into account when drawing up the inventory data.

3.1. Goal and Scope

Cradle-to-gate LCA analysis was modeled to understand the life cycle impact associated with the FSD process.

Consequently, a comparative analysis between the FSD and FSAM processes was conducted, with the aim of achieving an identical functional unit for both processes.

The LCA analysis seeks to compare the energy consumption and material usage of FSD and pinless FSAM.

In order to carry out the pinless FSAM process, metal sheets with a width larger than that of the wall to be obtained are required, to ensure correct stability through clamping systems.

3.2. Functional unit

Figures 3a and 3b show the chosen functional unit (the mass of the build with 100 mm x 14 mm x 10 mm (L x W x H) dimensions) for FSD and pinless FSAM setups, respectively. This choice is driven by the size of the consumable rotating tool of the FSD approach.

3.3. System boundary and Life Cycle Inventory (LCI)

The adopted system boundaries for the analyzed processes are reported in Figure 4: (a) material phase, manufacturing phase to obtain rotating consumable tools, manufacturing phase for FSD and finishing milling operation; (b) material phase, manufacturing phase to obtain metal sheet, manufacturing phase for FSAM and finishing milling operation.

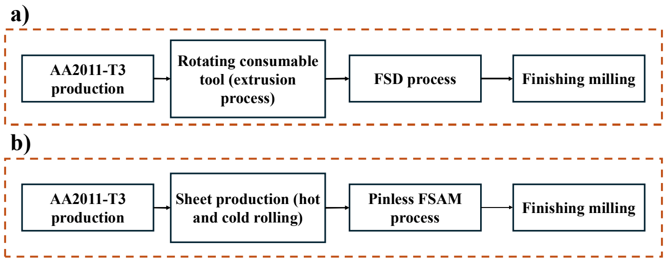

Fig. 4. System boundaries for (a) FSD and (b) Pinless FSAM.

Regarding the material phase, a portion of the modeling efforts was focused on the sheet and rod production manufacturing phase. Following the Recycled Content approach [16], it was assumed that a fraction (R=45%) of the aluminum input is sourced from secondary production [17]. Consequently, the system boundaries encompass an initial ingot comprising 55% primary production material and 45% secondary production material. The secondary production, involving the remelting of scrap, was modeled using data from the European Aluminum Environmental Profile Report [18]. To consider permanent losses due to oxidation during scrap remelting, an extra 16% of primary aluminum was incorporated [19].

Table 1. The set of data recorded during the manufacturing process.

	Pinless FSAM	FSD
Quantity of consumable tools [Pcs]	-	5
Quantity of metal sheets [Pcs]	10	-
Weight of a consumable tool [g]	-	98
Weight of a metal sheet [g]	36.5	-
Weight of single deposited layer [g]	36.5	28
Energy consumption for single deposition [kWh/layer]	0.2	0.07
Energy consumption for finishing milling [kWh/functional unit]	0.277	0.05
Total amount scrap [g]	325.9	451.1
Vertical load [kN]	6	9
Feed rate [mm/min]	80	370
Tool rotation speed [RPM]	1100	840

The extrusion and sheet production inventory were modeled by using the data available from the European Aluminum Association (EAA) [18]. For each step, all the energies and material flows (including process scrap) have been taken into account. Table 1 collects data recorded directly during the process. Where data was unavailable, data from Ecoinvent and data from literature were employed, such as machining energy consumption [20]. The selected process parameters for both processes were chosen with the aim to reduce the energy demand while still providing sound manufactured walls.

3.4. Interpretation of the results

The results computed for LCA analysis are shown in this section. In Table 2, the results characterized with ReCiPe2016 Midpoint (H) methodology are presented. The method assesses environmental impacts by quantifying 18 midpoint categories, giving detailed insight into specific environmental processes [21].

Table 2. ReCiPe2016 (H) Midpoint characterized comparative results.

Impact category	Pinless FSAM	FSD
GW [kg CO2 eq]	4.58E+00	4.40E+00
SOD [kg CFC11 eq]	2.29E-06	1.73E-06
IR [kBq Co-60 eq]	5.00E-01	4.75E-01
OF, HH [kg NOx eq]	9.57E-03	9.75E-03
FPMF [kg PM2.5 eq]	7.87E-03	8.44E-03
OF, TE [kg NOx eq]	9.69E-03	9.86E-03
TA [kg SO2 eq]	2.07E-02	2.15E-02
FEU [kg P eq]	1.76E-03	1.90E-03
MEU [kg N eq]	1.37E-04	1.50E-04
TE [kg 1,4-DCB]	4.85E+00	4.80E+00
FEC [kg 1,4-DCB]	1.75E-01	1.90E-01
MEC [kg 1,4-DCB]	2.37E-01	2.58E-01
HCT [kg 1,4-DCB]	9.88E-01	1.24E+00
HNCT [kg 1,4-DCB]	4.52E+00	5.11E+00
LU [m2a crop eq]	7.95E-02	5.29E-02
MRS [kg Cu eq]	6.80E-02	8.62E-02
FRS [kg oil eq]	1.22E+00	1.12E+00
WC [m3]	9.62E-02	1.02E-01

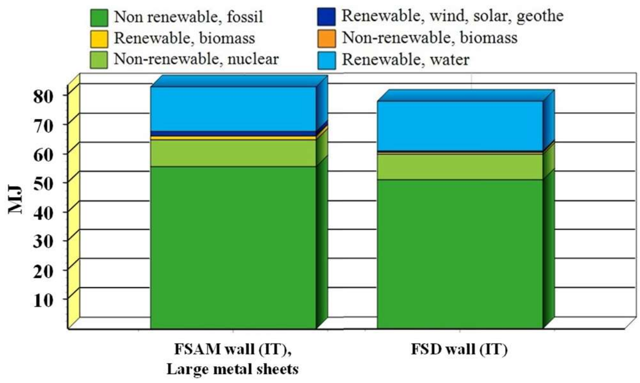

Fig. 5. Comparative CED results.

In order to provide clarity, some single-score indicators are now analyzed. In Figure 5, the Cumulative Energy Demand (CED) results are reported. The CED method evaluates the total primary energy demand, which is categorized by the sources of fossil, renewable, and nuclear energy. FSAM is characterized by a higher value of CED demand; moreover, it is possible to note that both processes exhibit a higher consumption of non-renewable energy sources. This outcome is due to the choice to consider the energy mix country as Italy.

The Recipe Endpoint (H) results are reported in Figure 6, despite the slight difference in mPt. Unlike what is observed for CED, here the FSAM exhibits better performance compared to FSD. Overall, it is possible to state that the two processes have a similar environmental impact, and this is also proved by analysis of the Midpoint category results (Table 3), where there is not a process that clearly outperforms the other.

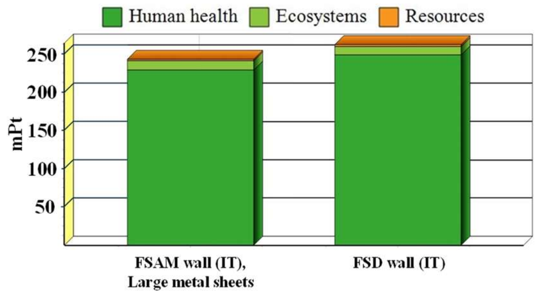

Fig. 6. ReCiPe2016 Endpoint (H) Characterization – comparative results.

To understand the contribution of each factor of influence towards the total impact, the tree representation for CED, provided by SimaPro, is reported in Figures 7 and 8.

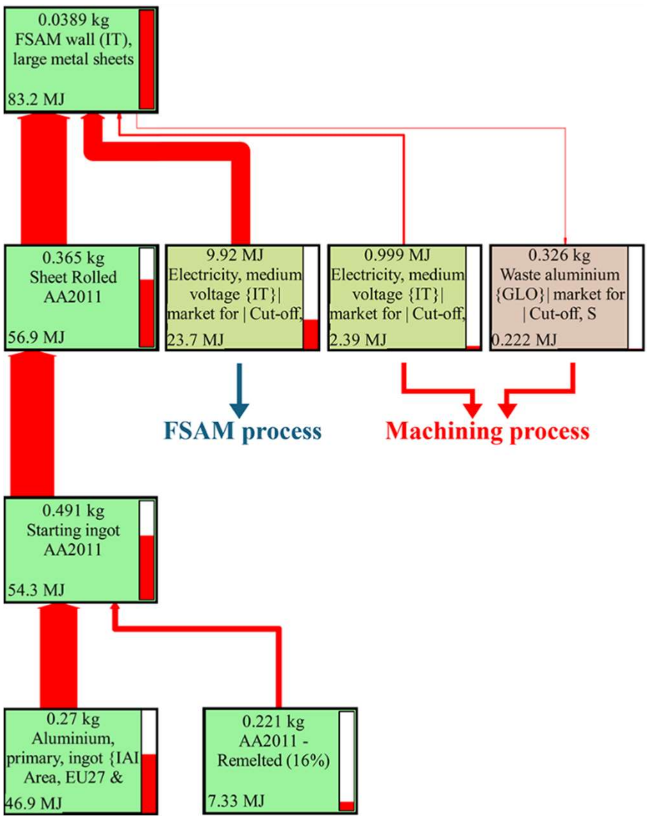

Fig. 7 Tree representation of CED for FSAM processes.

It is possible to note that for both processes, the material-related impact is the dominant factor. In fact, it accounts for 72% and 95% of the total CED for the FSAM and FSD, respectively, which is visible in the tree representation. On the other hand, when analyzing the electrical energy demand for the processing step, the pinless FSAM process proves to be more energy-consuming instead.

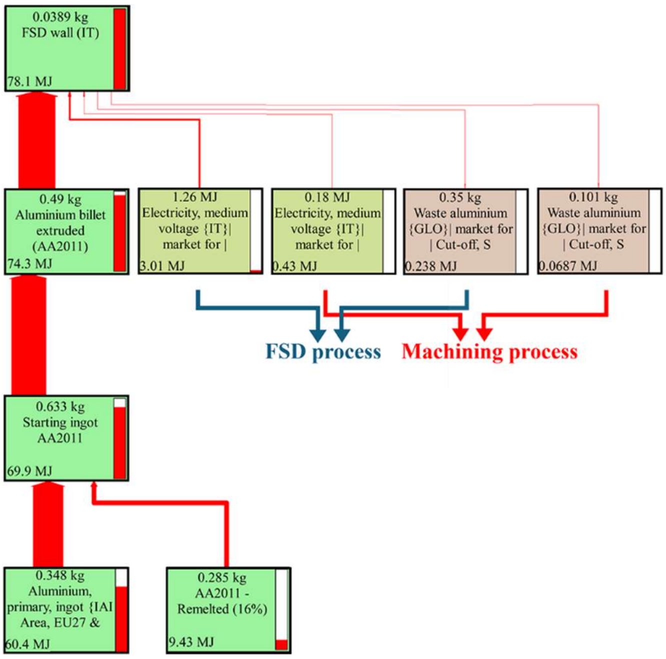

Fig. 8 Tree representation of CED for FSD processes.

In this way, the environmental performance of both processes is badly affected by the large amount of used material. To reduce the impact of material waste in a case of FSD, the optimization of tool size can be suggested. By changing the length and/or diameter of tools, it should be possible to minimize the undeposited amount of material depending on a target length of the layer. In a case of FSAM, this impact comes from the sheet area to be used for its clamping.

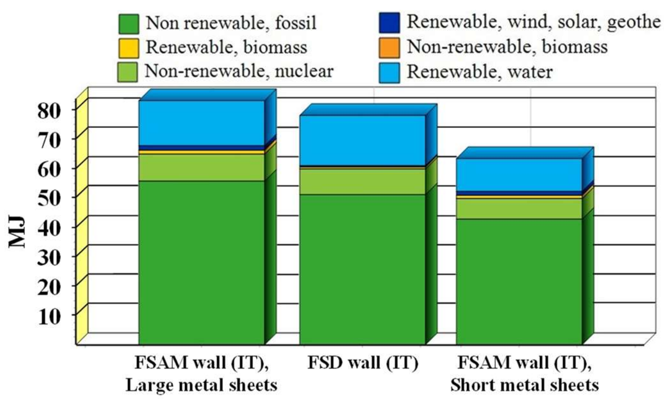

Fig. 8. Comparative CED results with possible upgrade.

In the present study, the used clamping is a lab-scale one and therefore, the clamping is not optimized for reducing the amount of used material. It is fair to assume that in an industrial environment, with dedicated fixtures and equipment, the portion of the sheet to be used for the clamping can be reduced significantly. In this respect, a further scenario was analyzed; to be more specific, the impact of using 50 mm wide sheets instead of 75 mm for the Pinless FSAM process has been evaluated. Comparative results are reported in Figure 8.

It is possible to note that the new Pinless FSAM configuration becomes the best solution in terms of CED performance.

4. Conclusions

In this study, FSD and Pinless FSAM processes were compared under the environmental impact angle.

Concerning the processing electrical energy, the FSAM requires a larger amount of energy than FSD. This is mainly due to the low feed rate value needed for obtaining a sound weld with a pinless tool.

LCA results reveal that the two processes are very close to each other in terms of environmental impact. It was observed that the material used for the additive manufacturing is the dominant factor contributing to Cumulative Energy Demand. To reduce the environmental impact, the process scrap minimization strategies were suggested. For the FSD, an optimization of the consumable rotating tool size to minimize the undeposited portion of it is strongly recommended. As far as the FSAM is concerned, process material scrap might be reduced by optimizing the clamping system to minimize the area of the metal sheet needed for the clamping.

Further development of the present study concerns the inclusion of new AM processes to the comparative analyses, such as Direct Energy Deposition approaches.

Acknowledgements

Part of this study was carried out within the activity of project using Italian MUR funds: “Aluminum Low Impact Circular Economy (ALICE)”, funded by the European Union - Next Generation EU, Mission 4 Component 1, Project: P2022WN727, CUP: B53D23027330001 PRIN 2022-PNRR.

References

[1] DebRoy T, Wei HL, Zuback JS, Mukherjee T, Elmer JW, Milewski JO, Beese AM, Wilson-Heid A, De A, Zhang W. Additive manufacturing of metallic components – Process, structure and properties. Prog Mater Sci 2018;92:112–224. https://doi.org/10.1016/J.PMATSCI.2017.10.001.

[2] Buffa G, Costa A, Palmeri D, Pollara G, Barcellona A, Fratini L. A new control parameter to predict micro-warping-induced job failure in LPBF of TI6AL4V titanium alloy. Int J Adv Manuf Technol 2023;126:1143–57. https://doi.org/10.1007/S00170-023-11179-6/FIGURES/14.

[3] Tuncer N, Bose A. Solid-State Metal Additive Manufacturing: A Review. JOM 2020;72:3090–111. https://doi.org/10.1007/s11837-020-04260-y.

[4] Rathee S, Srivastava M, Pandey PM, Mahawar A, Shukla S. Metal additive manufacturing using friction stir engineering: A review on microstructural evolution, tooling and design strategies. CIRP J Manuf Sci Technol 2021;35:560–88. https://doi.org/10.1016/J.CIRPJ.2021.08.003.

[5] Shao J, Samaei A, Xue T, Xie X, Guo S, Cao J, MacDonald E, Gan Z. Additive friction stir deposition of metallic materials: Process, structure and properties. Mater Des 2023;234:112356. https://doi.org/10.1016/J.MATDES.2023.112356.

[6] Zhao Z, Yang X, Li S, Li D. Interfacial bonding features of friction stir additive manufactured build for 2195-T8 aluminum-lithium alloy. J Manuf Process 2019;38:396–410. https://doi.org/10.1016/J.JMAPRO.2019.01.042.
[7] Gandra J, Krohn H, Miranda RM, Vilaça P, Quintino L, Dos Santos JF. Friction surfacing—A review. J Mater Process Technol 2014;214:1062–93. https://doi.org/10.1016/J.JMATPROTEC.2013.12.008.
[8] Kumar Srivastava A, Kumar N, Rai Dixit A. Friction stir additive manufacturing – An innovative tool to enhance mechanical and microstructural properties. Mater Sci Eng B 2021;263:114832. https://doi.org/10.1016/J.MSEB.2020.114832.
[9] Farabi E, Babaniaris S, Barnett MR, Fabijanic DM. Microstructure and mechanical properties of Ti6Al4V alloys fabricated by additive friction stir deposition. Addit Manuf Lett 2022;2:100034. https://doi.org/10.1016/J.ADDLET.2022.100034.
[10] Palanivel S, Nelaturu P, Glass B, Mishra RS. Friction stir additive manufacturing for high structural performance through microstructural control in an Mg based WE43 alloy. Mater Des (1980-2015) 2015;65:934–52. https://doi.org/10.1016/J.MATDES.2014.09.082.
[11] Hassan A, Pedapati SR, Awang M, Soomro IA. A Comprehensive Review of Friction Stir Additive Manufacturing (FSAM) of Non-Ferrous Alloys. Materials (Basel) 2023;16. https://doi.org/10.3390/ma16072723.
[12] Priarone PC, Campatelli G, Montevecchi F, Venturini G, Settineri L. A modelling framework for comparing the environmental and economic performance of WAAM-based integrated manufacturing and machining. CIRP Ann 2019;68:37–40. https://doi.org/10.1016/J.CIRP.2019.04.005.
[13] Pusateri V, Olsen SI, Hauschild MZ, Kara S. Potential for absolute sustainability of Wire-Arc Additive Manufacturing: A boat propellers case. CIRP Ann 2023;72:29–32. https://doi.org/10.1016/J.CIRP.2023.04.034.
[14] Saade MRM, Yahia A, Amor B. How has LCA been applied to 3D printing? A systematic literature review and recommendations for future studies. J Clean Prod 2020;244:118803. https://doi.org/10.1016/J.JCLEPRO.2019.118803.
[15] European Commission. International Reference Life Cycle Data System (ILCD) Handbook - General guide for Life Cycle Assessment - Provisions and Action Steps. Publications Office of the European Union: Luxembourg 2010:150. https://doi.org/10.2788/94987.
[16] Hammond G, Jones C, Lowrie F, Tse P, Building Services Research and Information Association., University of Bath. Embodied carbon: the Inventory of Carbon and Energy (ICE). BSRIA; 2011.
[17] Granta Design Limited 2023. https://www.ansys.com/it-it/products/materials/granta-edupack (accessed July 26, 2024).
[18] European Aluminum. Environmental Profile Report 2018. https://www.european-a luminium.eu/resource-hub/environmental-profile-report-2018/ (accessed July 17, 2024).
[19] Duflou JR, Tekkaya AE, Haase M, Welo T, Vanmeensel K, Kellens K, Dewulf W, Paraskevas D. Environmental assessment of solid state recycling routes for aluminium alloys: Can solid state processes significantly reduce the environmental impact of aluminium recycling? CIRP Ann 2015;64:37–40. https://doi.org/10.1016/J.CIRP.2015.04.051.
[20] Kara S, Li W. Unit process energy consumption models for material removal processes. CIRP Annals 2011;60:37–40. https://doi.org/10.1016/J.CIRP.2011.03.018.
[21] Huijbregts MAJ, Steinmann ZJN, Elshout PMF, Stam G, Verones F, Vieira M, Zijp M, Hollander A, van Zelm R. ReCiPe2016: a harmonised life cycle impact assessment method at midpoint and endpoint level. International Journal of Life Cycle Assessment 2017;22:138–47. https://doi.org/10.1007/s11367-016-1246-y.